5-Femtosecond Laser-Electron Synchronization for Pump-Probe Crystallography and Diffraction

Matthew Walbran,[1,2] Alexander Gliserin,[1,2] Kwangyun Jung,[3] Jungwon Kim,[3,*] and Peter Baum[1,2,†]

[1]*Ludwig-Maximilians-Universität München, Am Coulombwall 1, 85748 Garching, Germany*
[2]*Max-Planck-Institute of Quantum Optics, Hans-Kopfermann-Strasse 1, 85748 Garching, Germany*
[3]*Korea Advanced Institute of Science and Technology (KAIST), Daejeon 305-701, Korea*

For improving the temporal resolution in ultrafast pump-probe electron or x-ray diffraction, we report a laser-electron synchronization concept via direct microwave extraction from the laser frequency comb combined with phase detection by fiber-loop interferometry, *in situ* drift correction via electron-energy analysis, and laser-electron streaking for final timing metrology. We achieve a laser-electron jitter below 5 fs (rms) integrated between 8 min and Nyquist period (400 ns). Slower drifts are also below 5 fs (rms) after active compensation. This result helps advance femtosecond crystallography with electrons or x rays to the regime of fundamental atomic-scale dynamics and light-matter interaction.

I. INTRODUCTION

All processes in materials and molecules are basically defined by the motion of atoms and electron densities from initial to final conformations. A movielike visualization requires, atomic resolution in space and time, i.e., picometers and femtoseconds [1,2], which is attempted with pump-probe diffraction. The dynamics of interest is initiated by femtosecond laser pulses and probed at a sequence of time delays via diffraction of ultrashort electron or x-ray pulses having subatomic wavelength. Seminal achievements with ultrafast electron diffraction [3–8] and free-electron-laser crystallography [9–11] have demonstrated the high potential of these approaches towards a 4D visualization.

In most experiments, however, the temporal resolution is limited by the pump-probe timing jitter at the diffraction sample, especially when postprocessing methods [12–14] are incompatible due to long single-pattern readout times. In condensed matter and molecules, the time resolution required for resolving the half-period of relevant phonons and normal modes is, depending on the signal-to-noise ratio, on the order of 10 fs full width at half maximum or 5 fs root-mean-square (rms). X-ray and extreme-ultraviolet free-electron lasers provide a rms pump-probe jitter of about 30 fs [15]; ultrafast electron diffraction provides a rms jitter of about 100 fs [12,13,16]. These values originate in part from imperfect laser-microwave synchronization and impede the study of fundamental light-induced dynamics with pump-probe diffraction.

Here we report the synchronization of energetic (0.5-μJ) laser pulses at a low–intermediate repetition rate (5 MHz) to a train of microwave-compressed electron pulses. The scheme

is applicable to bright [2] and dim [17] electron pulses likewise. The laser is intense enough for sample excitation [17], and the electron pulses provide a 0.08-Å de Broglie wavelength for atomic-resolution diffraction from organic materials [18]. We demonstrate a laser-electron jitter of less than 5 fs (rms), integrated from approximately 8 min (2 mHz) to the Nyquist frequency (2.5 MHz). This is achieved by combining four synchronization and metrology concepts with individual advantages in certain frequency ranges. First, we implement an optical repetition-rate enhancer [19] to reduce the influence of thermal noise when detecting the timing of low-repetition-rate lasers in the microwave domain. Second, we precisely characterize the laser-microwave phase with a fiber-loop optical mixer [20,21] adapted for operation around the 800-nm laser wavelength of common Ti:sapphire pump lasers. Third, we introduce *in situ* drift diagnostics by electron-energy analysis, which provides the laser-electron timing directly within the microwave cavity that is used for bunch compression. Fourth, we apply laser-streaking electron-pulse metrology [22] at the location of a diffraction sample for out-of-loop verification. This unique combination of techniques allows selective identification and compensation of a few-femtosecond jitter over 9 orders of magnitude in frequency. The concept seems generally applicable, for example, to ultrabright electron diffraction [2], femtosecond crystallography with free-electron lasers [9,10], streak-camera applications [23,24], and time-resolved electron microscopy [6,25].

II. OPTICALLY ENHANCED DIRECT MICROWAVE EXTRACTION FROM THE LASER

Figure 1 depicts the experiment. The laser system is a long-cavity laser oscillator [26] providing 50-fs pulses

*jungwon.kim@kaist.ac.kr
†peter.baum@lmu.de

around 800-nm wavelength at a repetition rate of 5.13 MHz (red). Femtosecond electron pulses (blue) with (depending on the amount of flux required) 0.1–10 electrons per pulse on a statistical average [27] are generated by photoelectric emission from a gold layer using frequency-tripled laser pulses at 266-nm wavelength. Such single-electron or few-electron pulses provide a very high transverse coherence [28] useful for pump-probe diffraction from complex materials [18] that can be repeatedly excited [17]. The electron pulses are accelerated to 25 keV in a static electric field of 8.3 kV/mm; a magnetic lens is used for collimation or focusing (not shown). The electrons traverse a TM_{010} microwave cavity operated at approximately 6.2-GHz resonance frequency [29] at the zero-crossing phase for temporal compression at the diffraction target [30]. In the space-charge regime, i.e., at hundreds of electrons or more per pulse, the final pulse duration is limited by irreversible expansions of the Liouville phase-space volume, but bright pulses tens of femtoseconds long are, nevertheless, predicted to be achievable at tolerable energy bandwidth and coherence [31,32]. In the absence of space charge, the electron pulses can reach few-femtosecond duration and below [28,33,34]. A prerequisite in both endeavors, however, is precise laser-electron jitter control.

The electron pulse compressor's microwave signal at $f_{\mathrm{microwave}} \approx 6.237$ GHz is directly derived from the 1216th harmonic of the laser repetition rate $f_{\mathrm{rep}} \approx 5.13$ MHz via a fast photodiode followed by filtering and amplification. This concept is entirely passive and avoids any feedback electronics. However, the photodiode's electrical output power [35,36] in the relevant comb mode is limited by thermal noise. We solve this problem with an optical repetition-rate enhancer in the form of a passive Fabry-Pérot cavity; see Fig. 1. This idea was reported before [19] and is now applied experimentally to laser-electron synchronization. Basically, each femtosecond laser pulse produces a decaying pulse train with a temporal spacing resonant to the microwave frequency. This effect concentrates the limited photocurrent from the photodiode into a narrow frequency range around $f_{\mathrm{microwave}}$ and produces a substantial enhancement of the extractable microwave power, in our experiment approximately 4000 times higher than the comb mode using direct detection. The output at $f_{\mathrm{microwave}}$ is -15 dBm, which is subsequently filtered and amplified, using two stages of extremely narrow-band band-pass filters (approximately 6 MHz) and low-noise solid-state microwave amplifiers. The final power of 2 W is well sufficient for electron pulse compression at energies of tens of kiloelectron volts [29]. Unwanted neighboring harmonics at $f_{\mathrm{microwave}} \pm f_{\mathrm{rep}}$ (6.237 GHz $\pm$ 5.1 MHz) are thereby suppressed by 15 dB. Inside the electron compression cavity, the sideband suppression increases to 30 dB due to the cavity's approximately 2-MHz resonance bandwidth [29].

The final electron pulse duration after microwave compression and their timing are characterized by laser
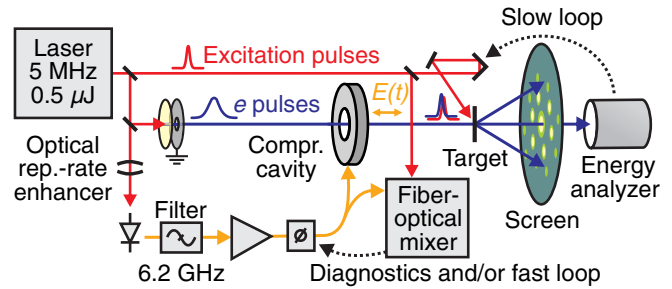

FIG. 1. Concept for laser-microwave synchronization at the 5-fs level (rms). A femtosecond long-cavity laser produces intense 800-nm excitation pulses (red) for pump-probe experiments. Electrons (blue) are generated via photoelectric emission and electrostatic acceleration. A microwave cavity compresses these pulses in time for pump-probe diffraction at a target. A laser-synchronized microwave (orange) is generated via passive optical repetition-rate enhancement and a fast photodiode, followed by filters and amplification. A fiber-loop optical phase detector monitors the performance with few-femtosecond precision up to Nyquist frequency. Energy analysis of the electron beam directly reveals the phase inside the cavity and, hence, the laser-electron synchronization directly at the diffraction target. A slow feedback loop or time stamping corrects for minute-scale timing drifts.

streaking [22]. Briefly, 25-keV electron pulses pass through a 50-nm-thin freestanding aluminum foil, while laser pulses are reflected from it. Thereby, the electrons gain or lose kinetic energy from the longitudinal component of the laser field, depending on the pump-probe delay. This interaction provides a laser-electron cross-correlation directly at the position of a diffraction target.

III. INTERFEROMETRIC FIBER-OPTICAL LASER-MICROWAVE DIAGNOSTICS AT 800 nm

High-frequency laser-microwave jitter characterization is achieved using a fiber-loop optical-microwave phase detector (FLOM PD) [20,21] adapted to cover the 800-nm spectral range of Ti:sapphire lasers. Figure 2(a) depicts the principle: the optical pulse train (red) is fiber coupled, passed through a circulator, and split via a 50:50 coupler; the two resulting pulse trains traverse a Sagnac-type fiber-loop interferometer in opposite directions. A bias unit provides $\pi/2$ phase shift between the clockwise and counterclockwise pulses for balanced detection on two photodiodes (green). The microwave (orange) copropagates with the clockwise optical pulses in a traveling-wave phase modulator, influencing the optical interference in dependence with the instantaneous microwave-field strength. The extreme sensitivity of optical interferometry produces superior resolution of the laser-microwave delay—down to attosecond precision has been demonstrated with low-noise fiber oscillators at 1550-nm telecommunication wavelength [21,37]. Other applications are

frequency metrology, microwave photonics, and time-frequency distribution [38–41].

Difficulties with applying the FLOM PD concept to laser pulses suitable for pump-probe experiments are their special wavelength (typically 800 nm), their ultrashort pulse duration (tens of femtoseconds), their low repetition rate (kilohertz to a few megahertz), and their wide spectral bandwidth (tens to hundreds of nanometers). Consequently, we must consider dispersion, nonlinear optical effects, amplitude-to-phase conversions, and spectral homogeneity for all involved components. The 800-nm FLOM PD uses fibers with a 4.9-μm mode-field diameter, a 5-μm fused 2×2 fiber splitter, a velocity-matched $LiNbO_3$-based phase modulator, multiorder achromatic wave plates and broadband Faraday rotators in the bias unit, attenuators based on mechanical mode distortion between fiber surfaces, and two silicon-based photodetectors. This optimization of spectral and dispersive characteristics comes at the cost of optical losses. The total optical efficiency from the fiber input to the balanced photodiodes is approximately 15%. The circulator's insertion loss causes intensity mismatch at the two interferometric output ports, making the system susceptible to microwave amplitude fluctuations. We solve this problem by placing an adjustable fiber attenuator before the respective photodiode. The input power has to be limited to approximately 40 mW to avoid nonlinear optical effects, which are noticeable at higher powers as intensity-dependent spectral broadenings after the fiber loop. Chirping the pulses can avoid these effects [42], but the pulse duration in the microwave modulator must stay sufficiently short.

With 40-mW incident optical power and 16 dBm of microwave power (approximately 40 mW), a phase-to-voltage coefficient of 3.25 V/rad or 0.13 mV/fs is achieved; see Fig. 2(b). Effectively, the FLOM PD is a microwave phase detector with unlimited frequency bandwidth; i.e., the laser-microwave delay can be measured for each single laser pulse. There are approximately 10^9 photons per laser pulse at the two diodes; this causes a shot-noise limit of about 0.2 fs (-170 dBc/Hz phase-noise floor) [21], plus technical noise. At the experimental conditions, but without microwave applied, the FLOM PD has a measured noise floor of -120 dBc/Hz at 10 Hz and -148 dBc/Hz at 1 MHz offset from the carrier frequency $f_{\mathrm{microwave}}$. This performance is slightly worse than demonstrated [21] and probably caused by the long-cavity laser's intensity noise of approximately 1% (rms) via residual or nonlinear amplitude-to-phase effects.

IV. TIME-OF-FLIGHT LASER-MICROWAVE PHASE DETECTOR

While the FLOM PD is capable of characterizing timing jitter over the entire relevant bandwidth up to the Nyquist frequency, it is insensitive to phase drifts originating apart from its microwave input. Specifically, temperature-related
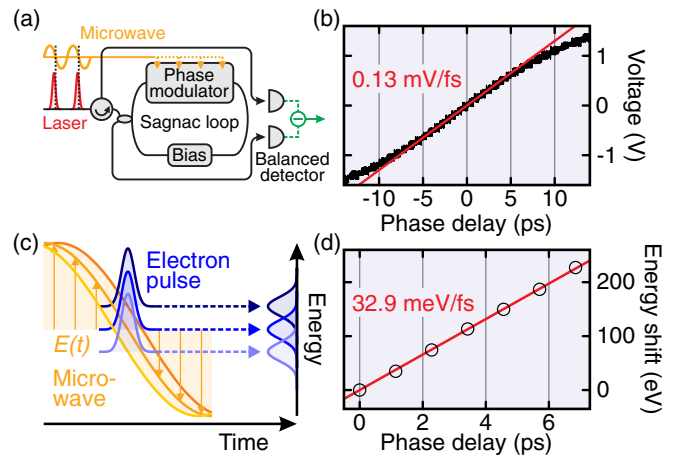

FIG. 2. Laser-microwave and laser-electron delay detection with few-femtosecond precision. (a) Fiber-loop optical-microwave phase detector (FLOM PD) adapted to intense Ti:sapphire laser pulses. The microwave (orange) changes the optical interference phase of a Sagnac loop; balanced detection (green) provides few-femtosecond resolution of laser-microwave jitter on a single-pulse basis. (b) Measured sensitivity of the 800-nm FLOM PD. (c) *In situ* laser-electron delay diagnostics using an energy analyzer. Phase delays in the compression cavity's microwave field (orange) directly increase or decrease the electron pulses' (blue) central energy. (d) Measured sensitivity.

timing drift inside the compression cavity is not measurable by any external phase detector. To solve this, an optical crystal can be placed inside the microwave compression cavity [12], but the measurement accuracy is only 30 fs (rms) [12], insufficient for our aims. Therefore, here we introduce *in situ* phase detection by energy analysis of the electron beam. Figure 2(c) depicts the concept: electron pulses passing through the microwave cavity at a time off the zero-crossing phase are subject to a change in central energy. This energy modulation can be understood as a streak camera in the longitudinal momentum domain. In the experiment, the energy analyzer is a homebuilt time-of-flight spectrometer for subrelativistic electron pulses providing single-shot capability at megahertz repetition rates and an energy resolution of better than 1 eV (full width at half maximum) over a range of approximately 10 eV at 25 keV [22]. Figure 2(d) shows the electron energy in dependence of a microwave delay deliberately induced with a mechanical phase shifter over a range of 6.8 ps or approximately 15° of the microwave phase. Around the maximum slope, a linear relation is observed with an energy-to-phase coefficient of $g_E = 33$ meV/fs. This results from the microwave field's amplitude and frequency and the cavity's geometry [29,43].

We call this approach a time-of-flight microwave phase detector. Its precision and highest measurement frequency is predominantly determined by the electron count rate. We use approximately 500 kHz, 10 times less than the laser repetition rate, in order to avoid double detections. Energy

spectra are integrated over a certain sampling interval, determining a trade-off between highest sampling rates (short intervals) and precise analysis (long intervals). We choose 2-s intervals for jitter contributions below 0.1 Hz and 100-ms intervals for contributions above 0.1 Hz. The accumulated energy spectra from every sampling interval are fitted by Gaussian functions in order to obtain their central energy, which is converted to timing drift using g_E. The fit accuracy given by a 95% confidence level is 2 fs (rms) for the 2-s intervals and 4.6 fs (rms) for the 100-ms intervals.

V. RESULTS AND JITTER CHARACTERIZATION OVER NINE FREQUENCY DECADES

Having established laser-microwave and laser-electron timing metrologies with few-femtosecond precision each, we now report a full characterization of residual jitter over nine decades of frequency. The optically enhanced passive synchronization scheme is free running; i.e., no feedback loop or stabilization technique is applied. Vibrations are minimized by rigid constructions. The number of electrons per pulse is set to 2 ± 2 on average [27], difficult to determine exactly but limited from below by the time-of-flight detector's count rate and from above by a camera measurement of the direct electron beam. Anyway, space charge is practically absent at such conditions, and the pulses are applicable to pump-probe diffraction of reversible condensed-matter processes [17].

Figure 3 shows an out-of-loop measurement of the microwave's single-sideband phase noise with respect to the laser-pulse train from 2 mHz (approximately 8 min) to the Nyquist frequency of 2.5 MHz. The high-frequency part (black) is derived from the FLOM PD's error signal by a spectrum analyzer. The result is multiplied by the compression cavity's transfer function, which constitutes a very narrow band-pass filter [29] that suppresses phase noise at high offset frequencies. For reference, the measured raw phase noise dominated by the FLOM PD's noise floor is shown as a gray line. The low-frequency trace (green) is obtained from an energy-analyzer measurement in the time domain and converted to phase noise by Fourier transformation. In the overlapping region, both phase detectors yield similar phase noise levels, confirming their independent calibrations. The integrated jitter in femtosecond units is plotted as the blue dashed line.

The combined result covering nine decades of frequency reveals several distinct behaviors of the synchronization scheme. Above 3 kHz, the measured phase noise is dominated by an essentially constant plateau at about −143 dBc/Hz, which is very similar to the FLOM PD's error signal with no microwave, i.e., its noise floor. The corresponding contribution to overall jitter is, therefore, an upper limit, and the scheme can actually perform better. At acoustic frequencies in the hertz to kilohertz range, there are some noticeable jitter contributions originating from mechanical vibrations and acoustic noise in the laboratory, but these have minimal contribution to overall jitter. The region of the most prominent acoustic noise between 280 and 460 Hz contributes only approximately 0.15 fs to the total jitter. On time scales in the seconds to minutes range, there are no more distinctive components, but the overall phase noise increases. The level at 1 min is −70 dBc/Hz. This low noise is a consequence of the superior stability of the laser repetition rate, which drifts by less than 1 Hz on a minute time scale and by less than 5 Hz over hours [29]. The 1216th harmonic of the repetition rate, hence, never leaves the centers of the involved filter elements, minimizing frequency-dependent phase drifts.

Total integration of Fig. 3 from the Nyquist frequency down to 2 mHz (approximately 8 min) yields a remarkable laser-microwave timing jitter of 4.8 fs (rms). This jitter is an upper limit due to the FLOM PD's noise floor in our experiment. Nevertheless, 4.8 fs (rms) is about 20 times better than in state-of-the-art ultrafast electron diffraction [12,13,16]. We mainly attribute this pleasant result to the
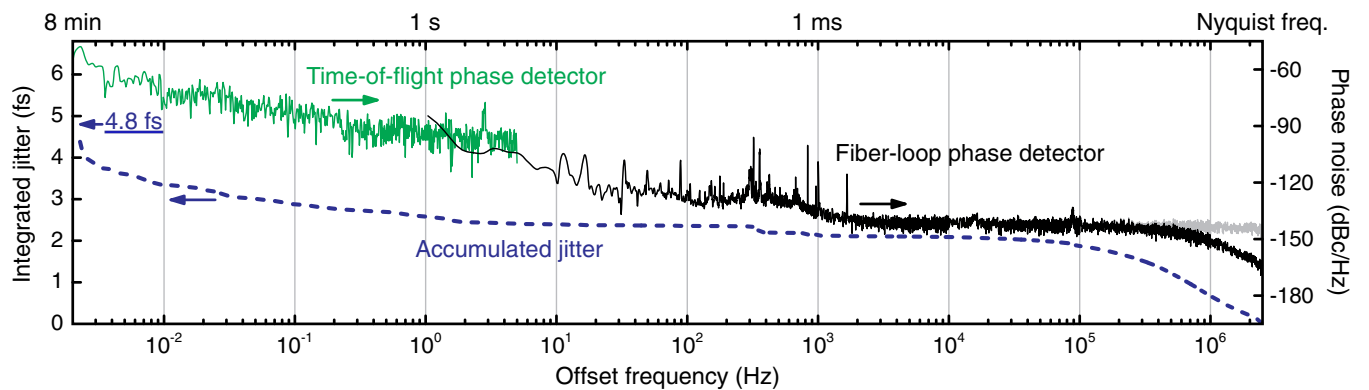

FIG. 3. Laser-electron jitter measured over nine decades of frequency. Jitter characterization using the fiber-loop interferometer (black) and the energy analyzer (green). The blue dashed line shows the accumulated jitter from Nyquist frequency down to an 8-min time scale, 4.8 fs in total.

purely passive synchronization scheme, where the microwave is directly derived from the laser-pulse train via optical repetition-rate enhancement, circumventing thermal noise problems. While our initial report of this approach [19] provides only a perspective, a rigorous out-of-loop characterization is demonstrated here.

We also attempt active stabilization using the FLOM PD in a delay-locked loop (dotted line in Fig. 1), but this does not improve the performance. The reason is our laser's intensity noise degrading the FLOM PD's noise floor. With active laser intensity control, carrier-envelope phase stabilization, and bias point tuning [44], attosecond-level feedback is, in principle, available [21,37,40], offering potential for yet another regime of jitter control.

VI. LONG-TERM DRIFT COMPENSATION

Despite the excellent stability on a time scale of minutes, synchronization unfortunately deteriorates on longer time scales (hours). Temperature drifts affect the optical repetition-rate enhancer, the compression cavity, the microwave amplifiers, sideband filters, the coaxial cabling [45], and the FLOM PD via changes of the laser parameters. The individual contributions can be identified using the *in situ* time-of-flight diagnostics with its few-femtosecond laser-electron-delay resolution. Figure 4 shows timing drift as a result of controlled temperature modulations at different components. The Fabry-Pérot resonator shows -3.2 fs/mK (left panel) caused by thermal expansion and shift of the resonance frequency, which, in turn, shifts the phase [19]. Under the mechanical cover, the temperature is stable to 11 mK (rms), but this still corresponds to a timing drift of 35 fs (rms) on long time scales. The microwave amplifiers have a temperature drift of 0.15 fs/mK (central panel). Fluctuating internal power dissipation causes slow temperature changes of 35 mK (rms) corresponding to a timing drift of approximately 5 fs (rms). The compression cavity's phase is temperature dependent with a linear coefficient of -1.1 fs/mK at resonance (right panel), due to expansion and contraction and corresponding shift of the resonance frequency. Water cooling provides
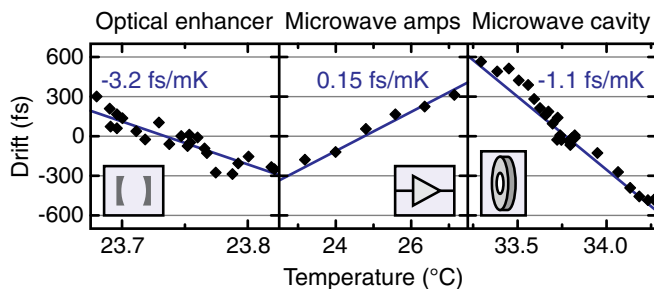

FIG. 4. Temperature-induced slow delay drifts caused by the optical repetition-rate enhancer, the microwave amplifiers, and the compression cavity.
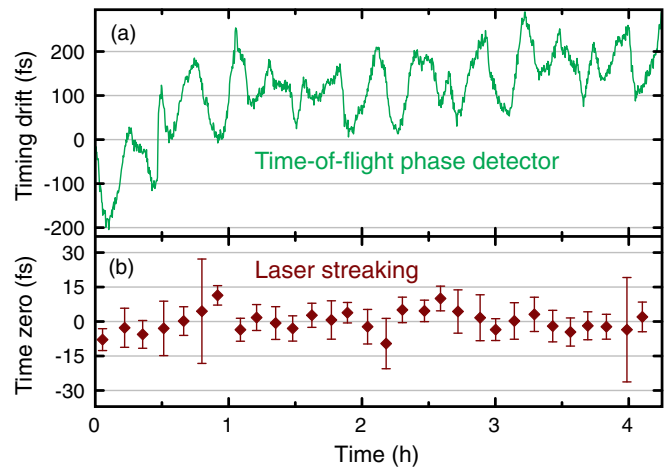

FIG. 5. Slow laser-electron timing drifts and their compensation. (a) Laser-electron delay recorded with the energy analyzer over 4 h. These data are used for time stamping. (b) Out-of-loop characterization of the final laser-electron drift at the diffraction target using laser-streaking pump-probe cross-correlation reveals sub-5-fs long-term stabilization.

approximately 35-mK (rms) stability, implying a slow timing drift of approximately 39 fs (rms).

Since <1 mK temperature stabilization is hardly feasible, here we report a different approach. In a proper experimental geometry, the time-of-flight phase detector is capable of continuously recording the direct beam while a diffraction experiment is performed, for example, with a hole or slit in the diffraction screen (see Fig. 1). Figure 5(a) shows the measured laser-electron timing drift over 4 h. As suspected from the calibrations above, the temperature oscillations in the laboratory induce laser-microwave timing drifts of about 200 fs, peak to peak. This online timing information is now available for a slow feedback loop or for data postprocessing. For demonstration, we choose the latter approach; out-of-loop characterization is achieved by pump-probe laser streaking at the location of the pump-probe diffraction target. One streaking scan takes about 8 min. Time zero, i.e., the overlap between electron and laser pulses, can be determined from the obtained laser-electron cross-correlation with an accuracy of approximately 7 fs. This accuracy is limited by the streaking laser-pulse duration of approximately 80 fs (full width at half maximum), constituting a dominant contribution to the cross-correlation width. Nevertheless, determination of time zero and its drifts is accurate enough using Gaussian fits to the cross-correlation's high-gain parts [22]. In order to measure timing drifts by time-of-flight energy analysis at the same time, the laser is periodically turned off with a shutter every few seconds.

Figure 5(b) shows the results. From the fitted time-zero positions (diamonds), we obtain statistical fluctuations of 4.7 fs (rms) over a measurement time of 4 h. Uncertainty in the streaking analysis by Gaussian fits [bars in Fig. 5(b)]

limits the out-of-loop characterization accuracy; the 4.7 fs (rms) is, therefore, an upper limit. Few-femtosecond laser-electron jitter can, therefore, be maintained at the location of a diffraction sample for arbitrarily long measurement times.

It is also interesting to determine the final compressed electron pulse duration, which is in the few-femtosecond regime according to simulations [29]. To this end, we apply laser streaking [22] and evaluate the cross-correlation width at highest-energy gains [22]. Deconvolution of these data with the streaking effect's Bessel-function-shaped temporal profile [46] and consideration of the geometrical distortions [47] produce an electron pulse duration of 12–35 fs (rms) or 28–80 fs (full width at half maximum). This duration is limited from above by the streaking measurement [22] and from below by pulse front aberrations in the electron beam, which are caused by the solenoid lenses used for beam transport. Here, the lenses are not completely "isochronic" [47] and not perfectly aligned [48], since the main purpose of this work is not electron pulse compression but jitter control. In another experiment, to be secured and reported elsewhere, we find some indications of significantly shorter electron pulses, thanks to the advancement in synchronization reported here.

VII. PERSPECTIVES

The final achievement, sub-5-fs jitter from 8 min to Nyquist frequency and sub-5-fs long-term drift, will help push pump-probe electron diffraction [3–8] to the regime of fundamental atomic motions on a few-femtosecond time scale, assuming short enough electron pulses [49]. This feat can help advance pump-probe diffraction approaches towards atomic resolution in space and time. We note that the reported synchronization concept is applicable to bright [2] and dim [17] electron pulses in a similar way. While space-charge effects might affect the electron pulse timing after photoemission and acceleration, the arrival time of the center of mass at the diffraction target is solely determined by the microwave field. The reported advances demonstrated here for few-electron pulses are, therefore, applicable to ultimately dense or bright electron pulses [2] as well, which will be crucial for irreversible or complex reactions [2]. We also believe that the reported synchronization scheme is useful for free-electron lasers, provided that the microwave power can be further increased. Amplification deteriorates the jitter level by approximately the square root of the noise figure. For example, a 100-W-class amplifier with 6-dB noise figure will increase the measured 5-fs jitter by a factor of approximately 2, still below 10 fs (rms). Higher-energy lasers at lower repetition rates can either directly drive an optical repetition-rate enhancer with optimized mirror reflectivities [19] or follow a reference laser via optical synchronization with few-femtosecond precision [50].

An alternative to jitter control is single-shot time stamping, i.e., measuring the drifting pump-probe delay for every pump-probe cycle [12–14]. However, depending on the laser repetition rate, the demand on the readout electronics is tremendous in this concept, because the time it takes to transfer a single-shot diffraction image to a computer system limits the amount of data that can be recorded. For many applications, it is, therefore, preferable to have jitter-free pump-probe synchronization with few-femtosecond precision, at least over some minutes, in order to integrate reasonably a diffraction pattern before readout. Such jitter performance is achievable with the synchronization scheme reported here.

Where are the limits? Amplitude-to-phase couplings in the photodiode can be avoided [51,52], monolithic design reduces the optical enhancer's susceptibility to frequency-dependent responses [19], and the laser's intensity noise can be stabilized to minimize amplitude-to-phase couplings in all applied components. The only fundamental limit seems to be how much optical power can be extracted at $f_{\text{microwave}}$ in comparison to thermal and quantum noise [53,54]; advanced diode concepts can help here. Alternatively, attosecond-level FLOM PD designs at Ti: sapphire wavelengths can provide an active feedback loop. With the reported progress, a promising route seems open to subfemtosecond laser-electron jitter and, given correspondingly short pump and probe pulses, subfemtosecond time resolution in atomic-scale electron and x-ray diffraction.

ACKNOWLEDGMENTS

[1] M. Chergui and A. H. Zewail, Electron and x-ray methods of ultrafast structural dynamics: Advances and applications, ChemPhysChem **10**, 28 (2009).

[2] R. J. D. Miller, Femtosecond crystallography with ultrabright electrons and x-rays: Capturing chemistry in action, Science **343**, 1108 (2014).

[3] H. Ihee, V. A. Lobastov, U. M. Gomez, B. M. Goodson, R. Srinivasan, C. Y. Ruan, and A. H. Zewail, Direct imaging of transient molecular structures with ultrafast diffraction, Science **291**, 458 (2001).

[4] B. J. Siwick, J. R. Dwyer, R. E. Jordan, and R. J. D. Miller, An atomic-level view of melting using femtosecond electron diffraction, Science **302**, 1382 (2003).

[5] P. Baum, D. S. Yang, and A. H. Zewail, 4D visualization of transitional structures in phase transformations by electron diffraction, Science **318**, 788 (2007).

[6] A. H. Zewail, Four-dimensional electron microscopy, Science **328**, 187 (2010).

[7] M. Eichberger, H. Schafer, M. Krumova, M. Beyer, J. Demsar, H. Berger, G. Moriena, G. Sciaini, and R. J. D. Miller, Snapshots of cooperative atomic motions in the optical suppression of charge density waves, Nature (London) **468**, 799 (2010).

[8] S. Wall, B. Krenzer, S. Wippermann, S. Sanna, F. Klasing, A. Hanisch-Blicharski, M. Kammler, W. G. Schmidt, and M. Horn-von Hoegen, Atomistic Picture of Charge Density Wave Formation at Surfaces, Phys. Rev. Lett. **109**, 186101 (2012).

[9] H. N. Chapman *et al.*, Femtosecond x-ray protein nanocrystallography, Nature (London) **470**, 73 (2011).

[10] J. Tenboer *et al.*, Time-resolved serial crystallography captures high-resolution intermediates of photoactive yellow protein, Science **346**, 1242 (2014).

[11] K. H. Kim *et al.*, Direct observation of bond formation in solution with femtosecond x-ray scattering, Nature (London) **518**, 385 (2015).

[12] G. J. H. Brussaard, A. Lassise, P. L. E. M. Pasmans, P. H. A. Mutsaers, M. J. van der Wiel, and O. J. Luiten, Direct measurement of synchronization between femtosecond laser pulses and a 3 GHz radio frequency electric field inside a resonant cavity, Appl. Phys. Lett. **103**, 141105 (2013).

[13] M. Gao, Y. Jiang, G. H. Kassier, and R. J. D. Miller, Single shot time stamping of ultrabright radio frequency compressed electron pulses, Appl. Phys. Lett. **103**, 033503 (2013).

[14] A. L. Cavalieri *et al.*, Clocking Femtosecond X Rays, Phys. Rev. Lett. **94**, 114801 (2005).

[15] S. Schulz *et al.*, Femtosecond all-optical synchronization of an x-ray free-electron laser, Nat. Commun. **6**, 5938 (2015).

[16] R. P. Chatelain, V. R. Morrison, C. Godbout, and B. J. Siwick, Ultrafast electron diffraction with radio-frequency compressed electron pulses, Appl. Phys. Lett. **101**, 081901 (2012).

[17] S. Lahme, C. Kealhofer, F. Krausz, and P. Baum, Femtosecond single-electron diffraction, Struct. Dyn. **1**, 034303 (2014).

[18] F. O. Kirchner, S. Lahme, F. Krausz, and P. Baum, Coherence of femtosecond single electrons exceeds biomolecular dimensions, New J. Phys. **15**, 063021 (2013).

[19] A. Gliserin, M. Walbran, and P. Baum, Passive optical enhancement of laser-microwave synchronization, Appl. Phys. Lett. **103**, 031113 (2013).

[20] J. Kim and F. X. Kärtner, Microwave signal extraction from femtosecond mode-locked lasers with attosecond relative timing drift, Opt. Lett. **35**, 2022 (2010).

[21] K. Jung and J. Kim, Subfemtosecond synchronization of microwave oscillators with mode-locked Er-fiber lasers, Opt. Lett. **37**, 2958 (2012).

[22] F. O. Kirchner, A. Gliserin, F. Krausz, and P. Baum, Laser streaking of free electrons at 25 keV, Nat. Photonics **8**, 52 (2014).

[23] G. H. Kassier, K. Haupt, N. Erasmus, E. G. Rohwer, H. M. von Bergmann, H. Schwoerer, S. M. M. Coelho, and F. D. Auret, A compact streak camera for 150 fs time resolved measurement of bright pulses in ultrafast electron diffraction, Rev. Sci. Instrum. **81**, 105103 (2010).

[24] C. M. Scoby, R. K. Li, E. Threlkeld, H. To, and P. Musumeci, Single-shot 35 fs temporal resolution electron shadowgraphy, Appl. Phys. Lett. **102**, 023506 (2013).

[25] A. Lassise, P. H. A. Mutsaers, and O. J. Luiten, Compact, low power radio frequency cavity for femtosecond electron microscopy, Rev. Sci. Instrum. **83**, 043705 (2012).

[26] S. Naumov, A. Fernandez, R. Graf, P. Dombi, F. Krausz, and A. Apolonski, Approaching the microjoule frontier with femtosecond laser oscillators, New J. Phys. **7**, 216 (2005).

[27] M. Aidelsburger, F. O. Kirchner, F. Krausz, and P. Baum, Single-electron pulses for ultrafast diffraction, Proc. Natl. Acad. Sci. U.S.A. **107**, 19714 (2010).

[28] P. Baum, On the physics of ultrashort single-electron pulses for time-resolved microscopy and diffraction, Chem. Phys. **423**, 55 (2013).

[29] A. Gliserin, A. Apolonski, F. Krausz, and P. Baum, Compression of single-electron pulses with a microwave cavity, New J. Phys. **14**, 073055 (2012).

[30] T. van Oudheusden, P. L. E. M. Pasmans, S. B. van der Geer, M. J. de Loos, M. J. van der Wiel, and O. J. Luiten, Compression of Subrelativistic Space-Charge-Dominated Electron Bunches for Single-Shot Femtosecond Electron Diffraction, Phys. Rev. Lett. **105**, 264801 (2010).

[31] T. van Oudheusden, E. F. de Jong, S. B. van der Geer, W. P. E. M. O. Root, O. J. Luiten, and B. J. Siwick, Electron source concept for single-shot sub-100 fs electron diffraction in the 100 kev range, J. Appl. Phys. **102**, 093501 (2007).

[32] S. Manz *et al.*, Mapping atomic motions with ultrabright electrons: Towards fundamental limits in space-time resolution, Faraday Discuss. **177**, 467 (2015).

[33] E. Fill, L. Veisz, A. Apolonski, and F. Krausz, Sub-fs electron pulses for ultrafast electron diffraction, New J. Phys. **8**, 272 (2006).

[34] L. Veisz, G. Kurkin, K. Chernov, V. Tarnetsky, A. Apolonski, F. Krausz, and E. Fill, Hybrid DC-AC electron gun for fs-electron pulse generation, New J. Phys. **9**, 451 (2007).

[35] K. Williams, R. Esman, and M. Dagenais, Effects of high space-charge fields on the response of microwave photodetectors, IEEE Photonics Technol. Lett. **6**, 639 (1994).

[36] D. Tulchinsky and K. Williams, Excess amplitude and excess phase noise of RF photodiodes operated in compression, IEEE Photonics Technol. Lett. **17**, 654 (2005).

[37] K. Jung, J. Shin, and J. Kim, Ultralow phase noise microwave generation from mode-locked Er-fiber lasers with subfemtosecond integrated timing jitter, IEEE Photonics J. **5**, 5500906 (2013).

[38] D. Hou, X. P. Xie, Y. L. Zhang, J. T. Wu, Z. Y. Chen, and J. Y. Zhao, Highly stable wideband microwave extraction by synchronizing widely tunable optoelectronic oscillator with optical frequency comb, Sci. Rep. **3**, 3509 (2013).

[39] B. Ning, S. Y. Zhang, D. Hou, J. T. Wu, Z. B. Li, and J. Y. Zhao, High-precision distribution of highly stable optical pulse trains with 8.8×10^{-19} instability, Sci. Rep. **4**, 5109 (2014).

[40] M. Y. Peng, A. Kalaydzhyan, and F. X. Kärtner, Balanced optical-microwave phase detector for sub-femtosecond optical-RF synchronization, Opt. Express **22**, 27102 (2014).

[41] X. Chen, J. Zhang, J. Lu, X. Lu, X. Tian, B. Liu, H. Wu, T. Tang, K. Shi, and Z. Zhang, Feed-forward digital phase

compensation for long-distance precise frequency dissemination via fiber network, Opt. Lett. **40,** 371 (2015).

[42] T. Ganz, V. Pervak, A. Apolonski, and P. Baum, 16 fs, 350 nJ pulses at 5 MHz repetition rate delivered by chirped pulse compression in fibers, Opt. Lett. **36,** 1107 (2011).

[43] P. L. E. M. Pasmans, G. B. van den Ham, S. F. P. Dal Conte, S. B. van der Geer, and O. J. Luiten, Microwave TM_{010} cavities as versatile 4D electron optical elements, Ultramicroscopy **127,** 19 (2013).

[44] M. Lessing, H. S. Margolis, C. T. A. Brown, P. Gill, and G. Marra, Suppression of amplitude-to-phase noise conversion in balanced optical-microwave phase detectors, Opt. Express **21,** 27057 (2013).

[45] K. Czuba and D. Sikora, Temperature stability of coaxial cables, Acta Phys. Pol. A **119,** 553 (2011).

[46] A. Feist, K. E. Echternkamp, J. Schauss, S. V. Yalunin, S. Schaefer, and C. Ropers, Quantum coherent optical phase modulation in an ultrafast transmission electron microscope, Nature (London) **521,** 200 (2015).

[47] C. Weninger and P. Baum, Temporal distortions in magnetic lenses, Ultramicroscopy **113,** 145 (2012).

[48] D. Kreier, D. Sabonis, and P. Baum, Alignment of magnetic solenoid lenses for minimizing temporal distortions, J. Opt. **16,** 075201 (2014).

[49] P. Baum, Towards ultimate temporal and spatial resolutions with ultrafast single-electron diffraction, J. Phys. B **47,** 124005 (2014).

[50] J. Kim, J. Chen, Z. Zhang, F. N. C. Wong, F. X. Kärtner, F. Loehl, and H. Schlarb, Long-term femtosecond timing link stabilization using a single-crystal balanced cross correlator, Opt. Lett. **32,** 1044 (2007).

[51] J. Taylor, S. Datta, A. Hati, C. Nelson, F. Quinlan, A. Joshi, and S. Diddams, Characterization of power-to-phase conversion in high-speed P-I-N photodiodes, IEEE Photonics J. **3,** 140 (2011).

[52] W. Zhang, T. Li, M. Lours, S. Seidelin, G. Santarelli, and Y. Le Coq, Amplitude to phase conversion of InGaAs pin photo-diodes for femtosecond lasers microwave signal generation, Appl. Phys. B **106,** 301 (2012).

[53] H. Jiang, J. Taylor, F. Quinlan, T. Fortier, and S. Diddams, Noise floor reduction of an Er:fiber laser-based photonic microwave generator, IEEE Photonics J. **3,** 1004 (2011).

[54] F. Quinlan, T. M. Fortier, H. Jiang, A. Hati, C. Nelson, Y. Fu, J. C. Campbell, and S. A. Diddams, Exploiting shot noise correlations in the photodetection of ultrashort optical pulse trains, Nat. Photonics **7,** 290 (2013).